

SMALL HYPERBOLIC POLYHEDRA

SHAWN RAFALSKI

Department of Mathematics and Computer Science
 Fairfield University
 Fairfield, CT 06824, USA
 srafalski@fairfield.edu

ABSTRACT. We classify the 3–dimensional hyperbolic polyhedral orbifolds that contain no embedded essential 2–suborbifolds, up to decomposition along embedded hyperbolic triangle orbifolds (turnovers). We give a necessary condition for a 3–dimensional hyperbolic polyhedral orbifold to contain an immersed (singular) hyperbolic turnover, we classify the triangle subgroups of the fundamental groups of orientable 3–dimensional hyperbolic tetrahedral orbifolds in the case when all of the vertices of the tetrahedra are non-finite, and we provide a conjectural classification of all the triangle subgroups of the fundamental groups of orientable 3–dimensional hyperbolic polyhedral orbifolds. Finally, we show that any triangle subgroup of a (non-orientable) 3–dimensional hyperbolic reflection group arises from a triangle reflection subgroup.

1. INTRODUCTION

Let P be a 3–dimensional hyperbolic Coxeter polyhedron, that is, a polyhedron in hyperbolic 3–space \mathbb{H}^3 all of whose dihedral angles are of the form π/n , where $n \geq 2$ is an integer. Then the group Γ of isometries of \mathbb{H}^3 generated by the reflections in the faces of P is a discrete group that acts on \mathbb{H}^3 with fundamental domain P . We denote by \mathcal{O}_P the quotient space obtained by identifying points of \mathbb{H}^3 by the action of the unique normal subgroup of Γ of index two. Then \mathcal{O}_P is an orientable hyperbolic 3–orbifold called a *hyperbolic polyhedral orbifold*. We call P a *hyperbolic reflection polyhedron*.

We classify the hyperbolic 3–dimensional polyhedral orbifolds that contain no embedded essential 2–suborbifolds, up to decomposition along embedded triangular 2–suborbifolds (see Figure 1):

Theorem 1.1. *A 3–dimensional hyperbolic polyhedron is small if and only if it is a generalized tetrahedron.*

We also determine those hyperbolic polyhedral orbifolds that contain an immersed (singular) hyperbolic triangular 2–suborbifold. This result is a generalization of the partial classification of triangle groups inside of arithmetic hyperbolic tetrahedral reflection groups given by Maclachlan [8]. In Section 4, we will provide a conjectural list of all the possibilities for immersed turnovers in all polyhedral orbifolds:

Date: January 2011.

Mathematics Subject Classification (2010): 52B10, 57M50, 57R18.

Key words and phrases. Hyperbolic polyhedra, 3–dimensional Coxeter polyhedra, triangle groups, hyperbolic orbifold, polyhedral orbifold, small orbifold, essential suborbifold, hyperbolic turnover.

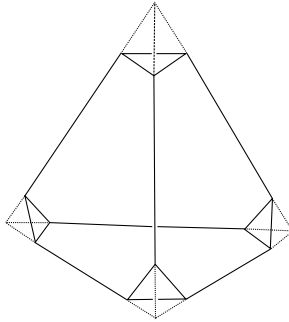


FIGURE 1. The small Coxeter polyhedra in \mathbb{H}^3

Theorem 1.2. *If a hyperbolic polyhedral 3-orbifold contains a singular hyperbolic turnover that does not cover an embedded hyperbolic turnover, then at least one component of its Dunbar decomposition is a generalized tetrahedron, and the immersed turnover is contained in a unique such component. Furthermore, if T is a generalized tetrahedron with all non-finite vertices and whose associated polyhedral 3-orbifold contains an immersed turnover, then, up to symmetry, T is of the form $T[2, m, q; 2, p, 3]$ (in the notation described in Section 4) with $m \geq 6$, $q \geq 3$ and $p \geq 6$, and the immersed turnover has singular points of orders m , q and p .*

We also determine the triangle subgroups of 3-dimensional hyperbolic reflection groups as arising from triangle reflection subgroups:

Theorem 1.3. *Any (orientable) triangle subgroup of a (non-orientable) 3-dimensional hyperbolic reflection group G arises as a subgroup of index two of a (non-orientable) triangle reflection subgroup of G .*

Essential surfaces play an integral role in low-dimensional topology and geometry. One of the most important instances of this fact is the proof of Thurston’s Hyperbolization Theorem for Haken 3-manifolds [16], [10]. In brief, Thurston’s Theorem is proved by decomposing a given 3-manifold M (which is called *Haken* if it contains an essential surface) along such surfaces as part of a finite-step process that ends in topological solid balls, from which the hyperbolic structure on M (whose existence is claimed by the theorem) is then, in a sense, reverse-engineered.

One difficulty that arises in attempting to extend the utility of essential surfaces to the orbifold setting is the possible presence of triangular hyperbolic 2-dimensional suborbifolds called *hyperbolic turnovers*. For example, whereas an irreducible 3-manifold with non-empty and non-spherical boundary always contains an essential surface, this is not always the case in the orbifold setting, with hyperbolic turnovers presenting the principal barrier. As a result, Thurston’s original definition of a Haken 3-orbifold [15, Section 13.5] has evolved somewhat over time. Theorem 1.1, which is proved using the observations that Thurston used to determine the original “non-Haken” polyhedral orbifolds, echoes Thurston’s original result with respect to this evolution of the language.

Acknowledgments. The author thanks Ian Agol for helpful conversations.

2. DEFINITIONS

There are several excellent references for orbifolds [4], [5]. All of the 3-orbifolds considered in this note are either hyperbolic polyhedral 3-orbifolds or the result of cutting a hyperbolic polyhedral 3-orbifold along a finite set of totally geodesic hyperbolic turnovers. A hyperbolic polyhedral 3-orbifold \mathcal{O}_P is geometrically just two copies of its associated hyperbolic polyhedron P with the corresponding sides of the two copies identified. Thus, \mathcal{O}_P is a complete metric space of constant curvature -1 except along a 1-dimensional singular subset which is locally cone-like. If P is compact, then \mathcal{O}_P is topologically a 3-sphere together with a trivalent planar graph (corresponding to the 1-skeleton of P) with each edge marked by a positive integer to represent the submultiple of π of the dihedral angle at the corresponding edge of P . If P is noncompact with finite volume, then its ideal vertices correspond to trivalent or quadrivalent vertices in the planar graph (again, corresponding to the 1-skeleton of P) and the sum of the reciprocals of the incident edge marks at each such vertex is equal to one. In this latter case, \mathcal{O}_P is topologically the result of taking a 3-sphere with this marked graph and removing a (closed) 3-ball neighborhood from each ideal vertex. The statements about the combinatorics of hyperbolic polyhedra in this paragraph are consequences of Andreev's Theorem [2], [3], [13], [15, Section 13.6], [7].

A (closed) 2-orbifold is topologically a closed surface with some finite set of its points marked by positive integers (greater than one). Every 2-orbifold can be realized as a complete metric space of constant curvature with cone-like singularities at the marked points, and where the sign of the curvature depends only on the topology of the underlying surface together with the markings. A 2-orbifold is called *spherical*, *Euclidean* or *hyperbolic* according to the sign of its constant curvature realization. A *turnover* is a 2-orbifold that is topologically a 2-sphere with three marked points, and a *hyperbolic turnover* is a turnover for which the reciprocal sum of the integer markings is less than one. Every embedded hyperbolic turnover in a hyperbolic 3-orbifold can be made totally geodesic by an isotopy in the 3-orbifold, and the preimage in \mathbb{H}^3 under the covering map of this totally geodesic 2-suborbifold is a collection of disjoint planes, each tiled by a hyperbolic triangle that is determined by the markings of the singular points (e.g., [9, Chapter IX.C], [1, Theorem 2.1]).

An embedded 2-suborbifold of \mathcal{O}_P is topologically a surface that meets the marked graph transversely. We note that any simple closed curve $C \subset \partial P$ that meets the 1-skeleton transversely determines a 2-suborbifold by adjoining to C the two topological disks that it bounds, one to either side of $\partial P \subset \mathcal{O}_P$. A closed path on ∂P that is isotopic to a simple circuit in the dual graph to the 1-skeleton of P is called a *k-circuit*, where k is the number of edges the path crosses.

The terminology of this paragraph is introduced in terms of general orbifolds. A compact *n-orbifold* \mathcal{O} with boundary is a metrizable topological space which is locally

diffeomorphic either to the quotient of \mathbb{R}^n by a finite group action or to the quotient of $\mathbb{R}^{n-1} \times [0, \infty)$ by a finite group action, with points of the latter type making up the *boundary* $\partial\mathcal{O}$ of \mathcal{O} (itself an $(n - 1)$ -orbifold). We use the term *orbifold ball* (respectively, *orbifold disk*) to refer to the quotient of a compact 3-ball (respectively, 2-disk) by a finite group action. We say a compact 3-orbifold \mathcal{O} is *irreducible* if every embedded spherical 2-suborbifold bounds an orbifold ball in \mathcal{O} . A 2-suborbifold $F \subset \mathcal{O}$ is called *compressible* if either F is spherical and bounds an orbifold ball or if there is a homotopically nontrivial curve in F that bounds an orbifold disk in \mathcal{O} , and *incompressible* otherwise. There is a relative notion of ∂ -incompressibility (whose exact definition we do not require). We call F *essential* if it is incompressible, ∂ -incompressible and not parallel to a boundary component of \mathcal{O} . We call a compact irreducible 3-orbifold *Haken* if it is either an orbifold ball, or a turnover crossed with an interval, or if it contains an essential 2-suborbifold but contains no essential turnover. A compact irreducible 3-orbifold is called *small* if it contains no essential 2-suborbifolds and has (possibly empty) boundary consisting only of turnovers. These definitions extend to any arbitrary 3-orbifold that is diffeomorphic to the interior of a compact 3-orbifold with boundary.

We observe that turnovers are always incompressible because they carry no homotopically nontrivial simple closed curves. As a consequence, in an irreducible 3-orbifold, any incompressible 2-orbifold (in fact, even any singular hyperbolic turnover) can be made disjoint from an embedded hyperbolic turnover.

It is a consequence of a theorem proved by Dunbar that a hyperbolic polyhedral 3-orbifold can be decomposed (uniquely, up to isotopy) along a system of essential, pairwise non-parallel hyperbolic turnovers into pieces that contain no essential (embedded) turnovers, and, moreover, that each component of the decomposition is either a Haken or a small 3-orbifold ([6], [4, Theorem 4.8]).

Definition 2.1. *A hyperbolic reflection polyhedron P is small if the Dunbar decomposition of \mathcal{O}_P consists of a single connected small component.*

In the projective model of \mathbb{H}^3 , consider a linearly independent set of four points, any or all of which may lie on the boundary of or outside of the projective ball. If the line segment between each pair of these points intersects the interior of the projective ball, then the points determine a *generalized tetrahedron*. This polyhedron is obtained by taking the (possibly infinite volume) polyhedron in \mathbb{H}^3 spanned by the points and truncating its infinite volume ends by the dual hyperplanes to the super-ideal vertices. The resulting polyhedron has finite volume and all of its vertices are either finite or ideal. The faces arising from truncated super-ideal vertices—which are called, along with the finite and ideal vertices, *generalized vertices*—are triangular, and the dihedral angle at each edge of these faces is $\pi/2$. In particular, if a generalized tetrahedron P is a Coxeter polyhedron, then any generalized vertex arising from a truncated face is a hyperbolic triangle that tiles (under the tiling associated to P) a geodesic plane in \mathbb{H}^3 , and thus gives rise to an embedded, one-sided hyperbolic turnover in \mathcal{O}_P .

3. PROOF OF THEOREM 1.1

Proof of 1.1. Let P be a 3-dimensional hyperbolic Coxeter polyhedron, and let \mathcal{O}_P be its hyperbolic polyhedral 3-orbifold. First assume that P is a generalized tetrahedron. Then \mathcal{O}_P is topologically the 3-sphere with a marked planar graph as in Figure 2. Each dot in the figure represents a generalized vertex, and so is

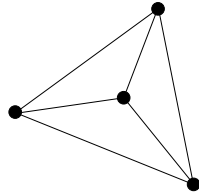


FIGURE 2. The graph associated to a generalized tetrahedron

either a finite vertex, a triangle or a Euclidean turnover (the latter if the vertex is ideal). Any dot that represents a triangle corresponds to a non-separating hyperbolic turnover of the Dunbar decomposition of \mathcal{O}_P . Moreover, since any two hyperbolic turnovers can be made disjoint by an isotopy, any other turnovers in the Dunbar decomposition occur as topological 2-spheres that intersect the graph from the figure in exactly three distinct edges. But the only possibility for such a 2-sphere is one that surrounds a dot, and that therefore is parallel to a generalized vertex of P . So the Dunbar decomposition of \mathcal{O}_P has a single component.

To see that this component is small, we consider the graph of Figure 2 as the 1-skeleton of a tetrahedron in the 3-sphere. Using standard topology arguments, it can be shown that an incompressible 2-suborbifold intersects the interior of this tetrahedron in triangles and quadrilaterals. But a triangular intersection implies that the incompressible 2-suborbifold is isotopic to the hyperbolic turnover associated to a generalized vertex, and a quadrilateral intersection produces a compression. So P is small if it is a generalized tetrahedron.

Now assume that P is small. The rest of the proof of Theorem 1.1 depends on the following simple observation [15, Proposition 13.5.2]:

Remark 1. Suppose that $C \subset P$ is a simple closed curve that is transverse to, forms no bigons with, does not surround a single vertex of, and that crosses at least two distinct edges of the 1-skeleton of P . Then C determines an incompressible 2-suborbifold of \mathcal{O}_P if and only if it never enters the same face twice and only enters adjacent faces along their common edge.

We begin with the following fact about triangles in ∂P :

Lemma 3.1. *If T is a triangle in ∂P , then T corresponds to a hyperbolic turnover in \mathcal{O}_P or P is a 3-simplex with possibly one generalized vertex.*

Proof of 3.1. Suppose that T is as in Figure 3a. If $1/p + 1/q + 1/r \geq 1$, then, by Andreev's Theorem, the three edges incident to the vertices of T must intersect (or

meet at a Euclidean turnover), in which case P is a tetrahedron (possibly with an ideal vertex). Otherwise, we have $1/p + 1/q + 1/r < 1$. Then the 3-circuit around this face determines a hyperbolic turnover in \mathcal{O}_P whose associated triangle in P must be boundary-parallel because P is small. The two possibilities are shown in Figures 3b and 3c. 3.1

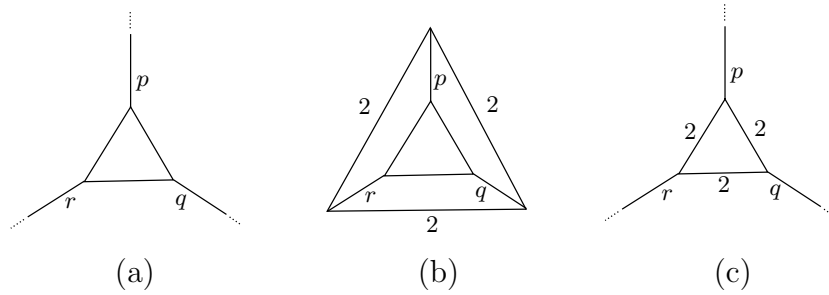


FIGURE 3. Triangular faces

Throughout the rest of the proof, we will use the observation from the above lemma, i.e., that any 3-circuit in a small hyperbolic polyhedron surrounds a generalized vertex.

Consider an n -sided face F of P , as in Figure 4. Assume that $n \geq 4$. The n -circuit

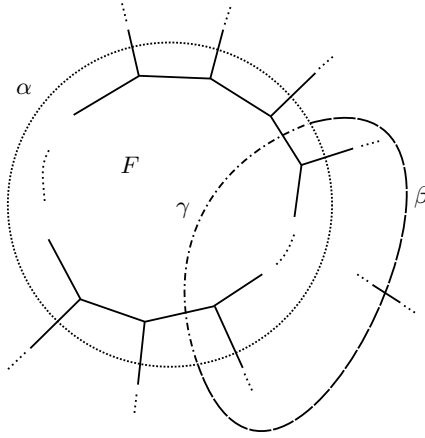


FIGURE 4. A face of P and a compression

α around F determines a 2-orbifold that must be compressible, with a compressing orbifold disk whose intersection with ∂P appears as the dashed arc β in the figure. Since $n \geq 4$, it must be that each side of the 3-circuit $\beta \cup \gamma$ contains at least two edges radiating outward from F (that is, edges meeting F only in vertices). Since \mathcal{O}_P is small, $\beta \cup \gamma$ therefore bounds a triangle $T \subset \partial P$. Figure 5 illustrates the two possibilities, depending on the side of $\beta \cup \gamma$ to which T lies. Of course, these differ only by the choice of projection of P into the plane.

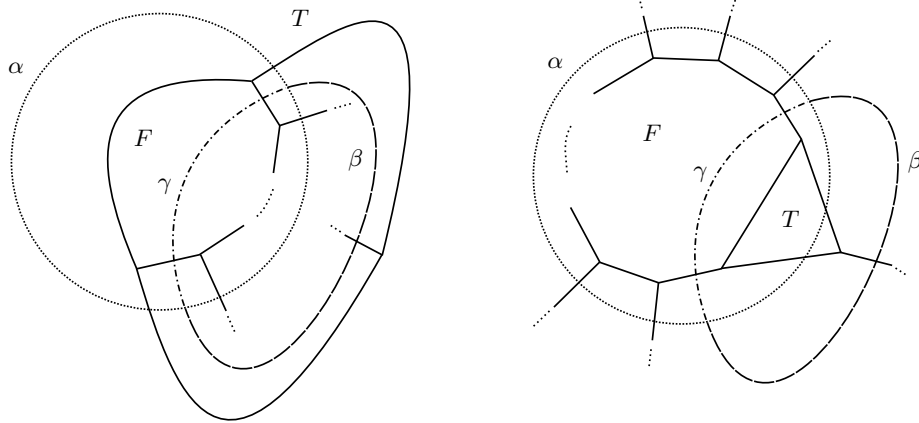


FIGURE 5. Two projections of a face of P with adjacent triangle

We now consider all such compressions of this 2-orbifold, and all of the resulting adjacent triangles to F . Let α denote the k -circuit that encloses F and these triangles, as in Figure 6.

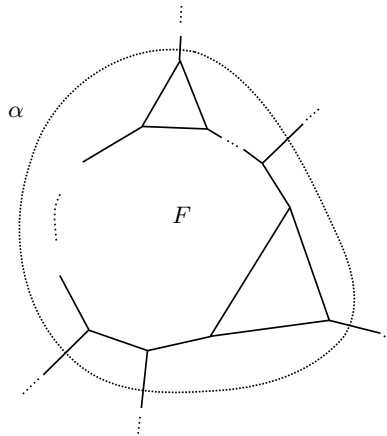


FIGURE 6. A face of P with all of its adjacent triangles, and a k -circuit

If $k = 2$, then F must be a quadrilateral with two triangles adjacent to it on opposite sides, in which case P is a triangular prism with one face that corresponds to a hyperbolic turnover in \mathcal{O}_P as in Lemma 3.1, i.e., P is a generalized tetrahedron. See Figure 7.

If $k = 3$, then α surrounds a generalized vertex to the outside. In this case, the face F must be as in Figure 8, where each dot represents either a finite vertex, an ideal vertex or a hyperbolic triangle. Filling in the generalized vertex to the outside of α , we have that P is a generalized tetrahedron.

If $k > 3$, then the 2-orbifold determined by α has a compression. But any such compression would add an adjacent triangular face to F , and we have assumed that

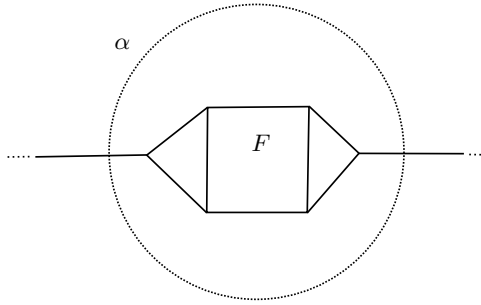


FIGURE 7. A face of P with all of its adjacent triangles, and a 2-circuit

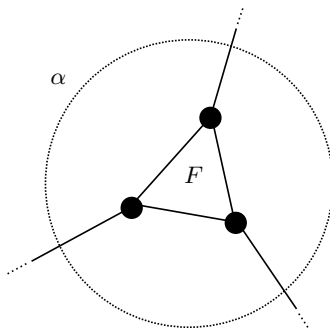


FIGURE 8. A face of P with all of its adjacent triangles, and a 3-circuit

α encloses all such triangles. So $k \leq 3$. This completes the proof. □ 1.1

4. TURNOVERS IN HYPERBOLIC POLYHEDRA

In this final section, we prove Theorems 1.2 and 1.3, and provide a classification of the immersed hyperbolic turnovers in those tetrahedral orbifolds that arise from tetrahedra with no finite vertices. Although Theorem 1.3 does not follow from Theorem 1.2, we will provide the proof of the former in the midst of the proof of the latter, as it contains an observation that is necessary for both proofs.

The author showed that if a hyperbolic 3-orbifold contains a singular hyperbolic turnover, then that turnover must be contained in a low-volume small 3-suborbifold [11]. In particular, we have the following

Theorem 4.1. *(Theorem 1.1 and Corollary 1.3 in [11]) Let Q be a compact, irreducible, orientable, atoroidal 3-orbifold. Then any immersion $f: \mathcal{T} \rightarrow Q$ of a hyperbolic turnover into Q is homotopic into a unique component of the Dunbar decomposition of Q , up to covers of parallel boundary components of the decomposition. Moreover, if f is a singular immersion that does not cover an embedded turnover or triangle, then the component containing $f(\mathcal{T})$ is unique, and it is a small 3-orbifold.*

Proof of 1.2. If \mathcal{O}_P is a hyperbolic polyhedral 3-orbifold, then it is homeomorphic to the interior of an orbifold that satisfies the hypotheses of Theorem 4.1. If \mathcal{O}_P contains a singular turnover, then this turnover is contained in a small component of the Dunbar decomposition of \mathcal{O}_P , and Theorem 1.1 classifies these small orbifolds as generalized tetrahedral orbifolds.

It remains to provide a classification of the generalized tetrahedra whose associated 3-orbifolds contain immersed turnovers. We will do so for generalized tetrahedra all of whose vertices are non-finite. *See the summary at the end of the paper for the results of the classification.* The techniques we use to provide this classification can be used to classify the immersed turnovers in all tetrahedral orbifolds, thereby extending and completing the classification begun by Maclachlan in the case of compact (non-generalized) tetrahedral orbifolds [8], however, the case-by-case analysis required to complete this classification in general is somewhat excessive.

We let $T[l, m, q; n, p, r]$ denote the hyperbolic generalized tetrahedron $ABCD$ with dihedral angles $\pi/l, \pi/m, \pi/q, \pi/n, \pi/p$ and π/r , as in Figure 9, with the convention that a vertex of T is truncated (respectively, ideal) if the dihedral angles of its three coincident edges sum to less than (respectively, equal to) π . The conditions on

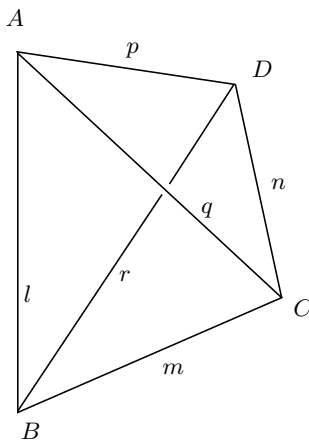


FIGURE 9. $T[l, m, q; n, p, r]$

l, m, q, n, p and r guaranteeing the existence of $T[l, m, q; n, p, r]$ are known [17]. In particular, there are nine compact (non-truncated) tetrahedra (e.g. [12, Chapter 7]), all of whose associated orbifolds contain singular turnovers. We note that, of the nine compact (non-truncated) tetrahedra, eight yield arithmetic hyperbolic 3-orbifolds. As we noted above, Maclachlan classified almost all of the immersed turnovers in these arithmetic tetrahedral orbifolds using arithmetic methods. Our geometric technique can be considered as an alternative means to prove (and extend) those results, without appeal to arithmeticity.

Denote by \mathcal{O}_T the 3-orbifold determined by $T[l, m, q; n, p, r]$. Recall from Section 2 that any hyperbolic turnover in a hyperbolic 3-orbifold may be assumed to be

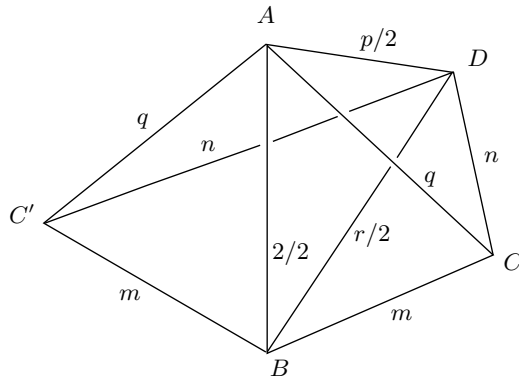
totally geodesic. It also follows from the incompressibility of hyperbolic turnovers in irreducible orbifolds that an immersed turnover must be disjoint from any embedded turnover [11, Lemma 5.3]. Consequently, an immersed hyperbolic turnover $f: \mathcal{T} \rightarrow \mathcal{O}_T$ lifts to the universal cover \mathbb{H}^3 as a collection of geodesic planes with some intersections—two or more of these planes will intersect whenever there is a covering transformation (i.e., an element of $\pi_1(\mathcal{O}_T)$) that does not move one plane completely disjoint from some of the others, and this must occur if there is a singular immersion of a turnover in \mathcal{O}_T —and, additionally, the collection of planes determined by an immersed turnover must be disjoint from the collection of planes determined by any turnover corresponding to a generalized vertex of T .

After these preliminaries, we now will prove Theorem 1.3.

Proof of 1.3. Let $P \subset \mathbb{H}^3$ be a polyhedron that generates the non-orientable 3-dimensional hyperbolic polyhedral reflection group G , and let $S \subset G$ be an orientable triangle subgroup. Then S is generated by two elliptic elements in G and stabilizes a plane $\Pi_S \subset \mathbb{H}^3$. In particular, Π_S meets the axis of every element of S at a right angle, and the intersections of Π_S with these axes comprise the vertex set of a tiling of Π_S by hyperbolic triangles. Every such vertex will have k lines passing through it (where k is the order of the elliptic element stabilizing the vertex) that are the perpendicular intersections with Π_S of G -translates of a side of P . This set of lines and their intersections generates a tiling of Π_S by hyperbolic triangles that, because triangle groups are maximal among the Fuchsian groups, covers the tiling associated to S . Therefore, S is contained in the corresponding triangle reflection subgroup of G . 1.3

We take a moment to emphasize the observation from the above proof: Any maximal (orientable) triangle subgroup of 3-dimensional hyperbolic polyhedral reflection group has as a fundamental domain a triangle whose sides are contained in the sides of the corresponding polyhedral tiling of \mathbb{H}^3 . This fact is used in the next paragraph.

Here is the strategy for classifying the immersed turnovers of \mathcal{O}_T (the proof is somewhat lengthy, but this paragraph contains the core idea): Consider a plane $\Pi_{\mathcal{T}}$ in the collection of planes in \mathbb{H}^3 corresponding to $f(\mathcal{T})$. This plane is stabilized by a copy of the fundamental group of some turnover (possibly a smaller turnover that is covered by $f(\mathcal{T})$, if the fundamental group of $f(\mathcal{T})$ is not maximal)—a subgroup of isometries of the fundamental group of the orbifold \mathcal{O}_T —for which there is a tiling of $\Pi_{\mathcal{T}}$ by hyperbolic triangles whose edges arise from the intersections of $\Pi_{\mathcal{T}}$ with $\pi_1(\mathcal{O}_T)$ -translates of the sides of T and whose vertices arise from the intersections of $\Pi_{\mathcal{T}}$ with $\pi_1(\mathcal{O}_T)$ -translates of the edges of T . We therefore begin at an arbitrary edge e_1 of T and develop copies of T in \mathbb{H}^3 along one of the faces at e_1 until we come to another edge e_2 in the development, at which point we check whether or not the three planes—one plane that meets only e_1 , one plane that meets only e_2 , one plane that meets both e_1 and e_2 —pairwise intersect at angles $\pi/a, \pi/b$ and π/c , where $1/a + 1/b + 1/c < 1$. These three intersections must occur along translates of the edges of T and therefore determine a triangle group. Along the way as we

FIGURE 10. Two copies of the tetrahedron $T[2, m, q; n, p, r]$

develop T through \mathbb{H}^3 , we will encounter translates of edges of T whose associated elliptic elements will yield immersions of $f(\mathcal{T})$ (because they will neither preserve the invariant plane of the triangle group nor translate it to be disjoint from itself), and after sufficient development this process can be shown to terminate.

We divide the remainder of the proof into subsections.

4.1. The case when a single edge separates e_1 from e_2 :

4.1.1. *The single separating edge has order 2:* To begin, we determine the case in which the immersed turnover can be found after crossing only one edge between e_1 and e_2 (there must be at least one edge crossed, in this process, to ensure that the turnover is not parallel to a vertex). Consider Figure 10, which shows two copies of the tetrahedron $T[2, m, q; n, p, r]$. Each edge is labeled according to the submultiple of π for the dihedral angle there (so, for example, the edge AD has a dihedral angle of $2\pi/p$). In particular, the points A, B, C and C' are coplanar. We use F to denote the face ABC of T and Π_F to denote the plane that contains F . We consider the edges $e_1 = AC'$ and $e_2 = BC$, and the planes $\Pi_1 = AC'D$, Π_F and $\Pi_2 = BCD$. Under the assumption that all of the vertices of T are non-finite, we observe it is necessary for m, q, p and r to all be at least 3. From the figure, we see that Π_1 meets Π_F at an angle of π/q and that Π_F meets Π_2 at an angle of π/m , and so we are left to determine whether or not Π_1 and Π_2 intersect, and at what angle this possible intersection occurs. The vertex D is either ideal or truncated. If it is ideal, then its link is the orbifold quotient of a horosphere by a Euclidean triangle group. If it is truncated, then it corresponds to a geodesic plane in the universal cover that is stabilized by a hyperbolic triangle group. In both cases, we illustrate the straightforward geometric determination of the conditions on n, p and r that ensure the intersection of Π_1 and Π_2 in the link of D , and determine the angle at which any intersection occurs [11, Section 9.4].

Consider Figure 11, which illustrates part of the link of D (this is either a hyperbolic plane or a Euclidean plane corresponding to the horosphere centered at an ideal vertex). The vertices in the picture are labeled according to the edges of T that are

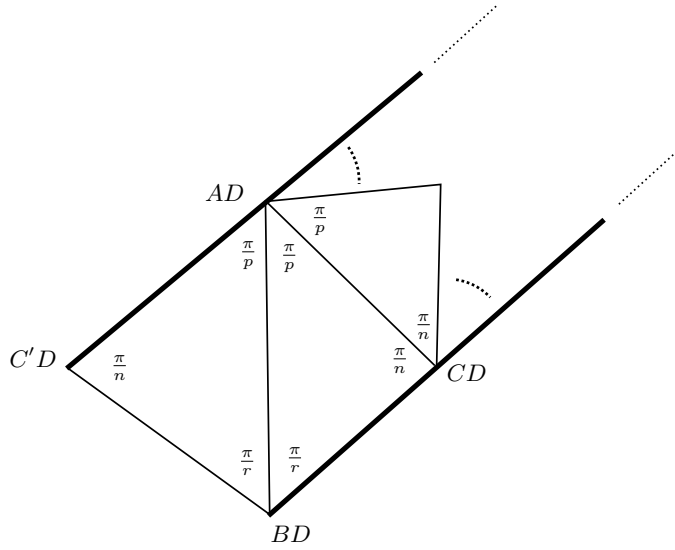


FIGURE 11. An illustration of part of the the link of a non-finite vertex of $T[2, m, q; n, p, r]$

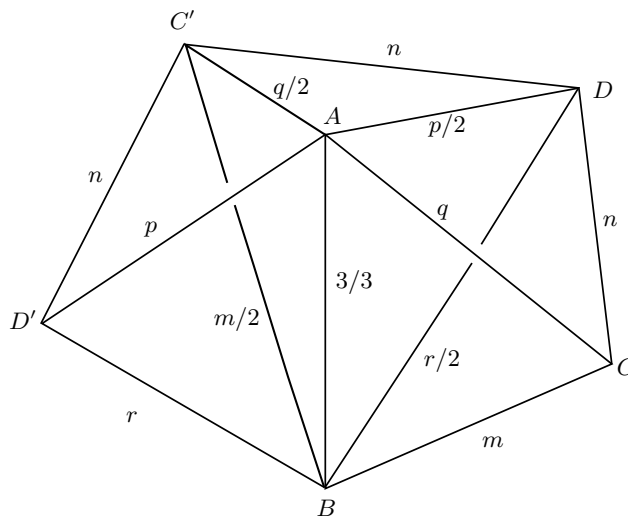
incident at D . If $n > 2$, we have (because r and p are both at least 3) the inequalities $(p - 2)\pi/p + (n - 1)\pi/n \geq \pi$ and $(r - 2)\pi/r + (n - 1)\pi/n \geq \pi$, and therefore the indicated bold lines (along with the corresponding planes Π_1 and Π_2) do not intersect. A similar argument implying that Π_1 and Π_2 do not intersect holds when $n = 2$ and both p and r are greater than three. Finally, if $n = 2$ and $p = 3$, then it is easily seen Π_1 and Π_2 intersect at an angle of π/r (or an angle of π/p if $n = 2$ and $r = 3$).

We therefore have, when $l = 2$ and our search for a turnover crosses only one edge, that an immersed turnover only arises when $n = 2$ and either $r = 3$ or $p = 3$. If $r = 3$, then this yields a triple of planes intersecting pairwise in angles of π/q , π/m and π/p , with $q \geq 3$, $m \geq 6$ and $p \geq 6$. If $p = 3$, then the pairwise angles of intersection are π/q , π/m and π/r , with $q \geq 6$, $m \geq 3$ and $r \geq 6$. (The inequalities are induced by the assumption that all of the vertices of T are non-finite.) By analyzing Table 1 (whose data is collected from Singerman [14]), we see that this triple of planes does not yield a triangle group that contains any other triangle group (compare the first column of the table with the second column). Also (comparing the second column with the first), we can see that this triple of planes does not yield a triangle group that is contained in a larger triangle group, for this would imply that the triangular fundamental domain formed by by these three planes would be visibly divided, in Figure 10, by triangles corresponding to the larger triangle group. Consequently, we conclude that the (q, m, p) or (q, m, r) triangle determined by Π_1 , Π_F and Π_2 is not parallel to (a cover of) any of the vertices of T , and therefore that it determines an immersed turnover in \mathcal{O}_T , because \mathcal{O}_T is small. These observations are summarized in items (1) and (2) at the conclusion of the paper.

4.1.2. *The single separating edge has order 3:* We next turn to the case in which the immersed turnover can be found after crossing only one edge between e_1 and e_2 ,

$T(l, m, n)$	$\geq T(p, q, r)$	Index	Normal
$(3, 3, t)$	(t, t, t)	3	Yes
$(2, 3, 2t)$	(t, t, t)	6	Yes
$(2, s, 2t)$	(s, s, t)	2	Yes
$(2, 3, 7)$	$(7, 7, 7)$	24	No
$(2, 3, 7)$	$(2, 7, 7)$	9	No
$(2, 3, 7)$	$(3, 3, 7)$	8	No
$(2, 3, 8)$	$(4, 8, 8)$	12	No
$(2, 3, 8)$	$(3, 8, 8)$	10	No
$(2, 3, 9)$	$(9, 9, 9)$	12	No
$(2, 4, 5)$	$(4, 4, 5)$	6	No
$(2, 3, 4t)$	$(t, 4t, 4t)$	6	No
$(2, 4, 2t)$	$(t, 2t, 2t)$	4	No
$(2, 3, 3t)$	$(3, t, 3t)$	4	No
$(2, 3, 2t)$	$(2, t, 2t)$	3	No

TABLE 1. Triangle Supergroups and Subgroups

FIGURE 12. Three copies of the tetrahedron $T[3, m, q; n, p, r]$

where the order of the crossed edge is $l = 3$. See Figure 12. Let $e_1 = AD'$, $e_2 = BC$, $\Pi_1 = AC'D'$ and $\Pi_2 = BCD$. We observe that, in order for Π_1 to intersect Π_2 , it is necessary that Π_2 cross at least one of the planes ABC' or ADC' . By considering the geometry of the generalized vertex B , we have that Π_2 meets ABC' if and only if $r = 2$. In this case, $\Pi_2 = BDC'$ (as planes) and Π_1 and Π_2 can therefore only intersect at C' . The conditions for intersection at C' are either $m = 2$ (not possible, since $r = 2$), or $n = 2$ and one of q or m equals 3 (not possible, since $r = 2$), or else

$q = 2$. In the last case, the intersection of Π_1 and Π_2 occurs along the edge $C'D$ at an angle of π/n , and because $q = 2 = r$ we must have $m \geq 6$, $p \geq 6$ and $n \geq 3$. In this case, $T = T[3, m, 2; n, p, 2]$ contains an immersed (m, n, p) turnover, and this tetrahedron (and the set of conditions on m, n and p) is symmetric to the tetrahedron in item (1) at the end of the paper (it is listed as item (3), additionally).

Otherwise, we have that Π_2 must intersect ADC' , and any possible intersection of Π_1 and Π_2 must occur on the side of ADC' opposite to vertex B . Using the geometry of the generalized vertex D , we conclude that either $r = 2$ (the case we just analyzed), or $p = 2$, or $n = 2$ and one of p or r equals 3. If $p = 2$, then $q \geq 6$ (using the vertex A), $n \geq 3$ (using the vertex D) and the angle sum of the angles formed by Π_1 and Π_2 with ADC' on the side opposite vertex B satisfies the inequality $(n-1)\pi/n + (q-2)\pi/q \geq \pi$. Since the lines AC' and CD are disjoint in the plane ADC' ($= ACDC'$), we conclude that $\Pi_1 \cap \Pi_2 = \emptyset$ in this case. (Note: we are using the fact that two planes that intersect a third plane in \mathbb{H}^3 , and that do not intersect in that third plane, can only meet, if at all, on the side of the third plane where the incident angles sum to less than π .)

In the remaining case, we have $n = 2$ and one of p or r equals 3. If $p = 3$, then $r \geq 6$ and q and m must both be bigger than 2 and also satisfy $1/q + 1/m \leq 1/2$. If we consider modifying Figure 12 by adjoining another copy of T to the face ACD , then it is readily seen that Π_2 meets the plane ADC' at an angle of $(r-1)\pi/r \geq 5\pi/6$ on the side of ADC' opposite to vertex B . The corresponding angle formed by Π_1 with ADC' (opposite to vertex B) is $(q-2)\pi/q \geq \pi/3$. Since $(r-1)\pi/r + (q-2)\pi/q > \pi$, we conclude that $\Pi_1 \cap \Pi_2 = \emptyset$ in this case. The case when $n = 2$ and $r = 3$ is entirely similar, with the same conclusion.

4.1.3. *The single separating edge has order greater than 3:* It remains for us to handle the analogous cases to the previous two cases, that is, when the search for an immersed turnover crosses a single edge between Π_1 and Π_2 , and when $l > 3$. We will show that no immersed turnovers can be found when $l > 3$.

We consider first the case when $l = 4$ and the vertex B has the Euclidean type $(2, 4, 4)$ with $m = 4$. Consider Figure 13, which illustrates the view in the upper half-plane model of \mathbb{H}^3 from the vertex B (which we have placed at the point at infinity), along with an accompanying diagram of four copies of T . Now Π_2 is represented in the diagram by the line CD . The plane Π_1 must be represented by a circle centered at some point in the triangle $AC''D'$ which meets each line segment AD' , AC'' and $C''D'$ (at angles of π/p , π/q and π/n , respectively) and which cannot contain the vertices of this triangle in its interior disk. Such a circle is depicted. Since such a circle cannot intersect the line CD , we conclude that $\Pi_1 \cap \Pi_2 = \emptyset$. An analogous argument can be used to show that we obtain no immersed turnover in this fashion, whenever the vertex B is Euclidean and l is not equal to 2 or 3.

We are left then to consider the case when $l \geq 4$ and the vertex B has a hyperbolic type. The argument is similar to the Euclidean vertex case, but we provide the details. Consider first the case of Figure 14. (This figure, along with the similar figures in this

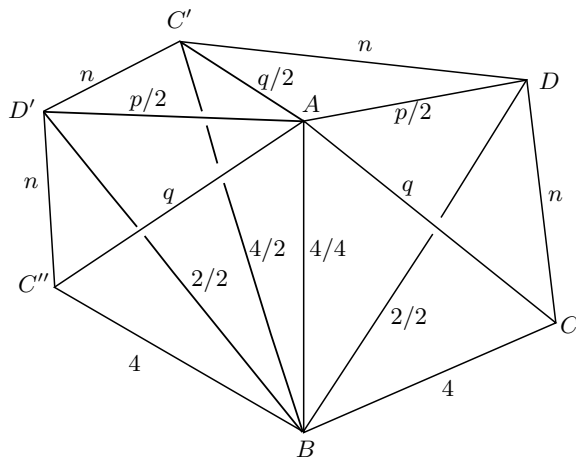
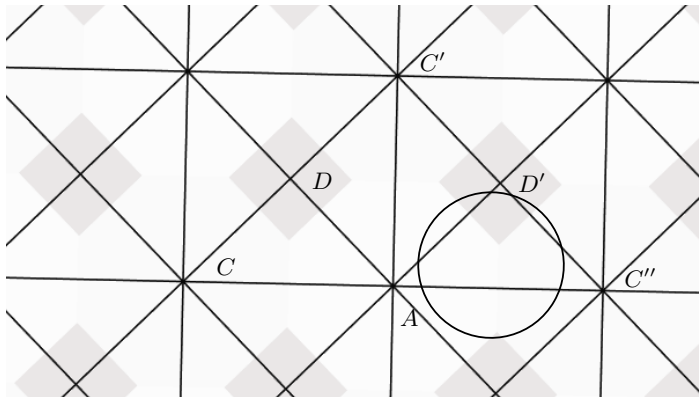


FIGURE 13. The view from the ideal vertex of type $(2, 4, 4)$.

section, was generated using the software *KaleidoTile* by Jeffrey Weeks [18].) For the purposes of illustration, we have assumed that vertex B has the type $(2, 4, 5)$, with $l = 5$, $m = 2$ and $r = 4$. If we consider the hyperbolic plane that truncates vertex B as a hemisphere in the upper half-plane model, then the Poincaré disk tiling pattern of the figure will result from projecting this hemisphere to the bounding plane of \mathbb{H}^3 through its nadir. In particular, as in the Euclidean vertex case, each line or semicircular arc in the figure represents a plane in the tiling of \mathbb{H}^3 by T (we have indicated five copies of T , labeled the endpoints of the lines emanating from B by the corresponding letters in the illustrated tiling, and applied an isometry so that A is at the center of the Poincaré disk), and the planes Π_1 and Π_2 are represented by a circle and the line CD , respectively. The circle representing Π_1 must, as in the previous case, intersect the line segments AC''' and AD'' (at angles of π/q and π/p , respectively), intersect the semicircular arc $C''D''$ (at an angle of π/n), have center contained in the hyperbolic triangle $AC''D''$ and must not contain A , C''' or

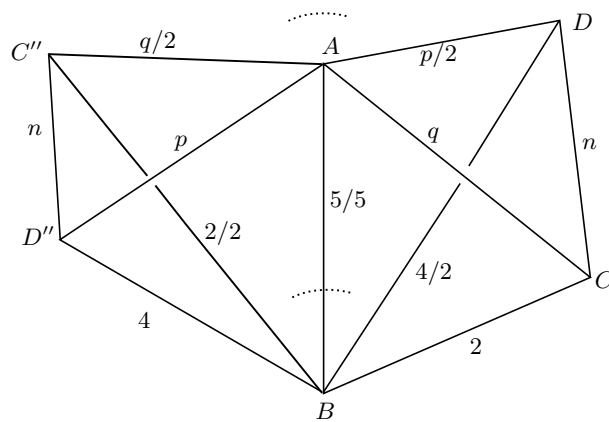
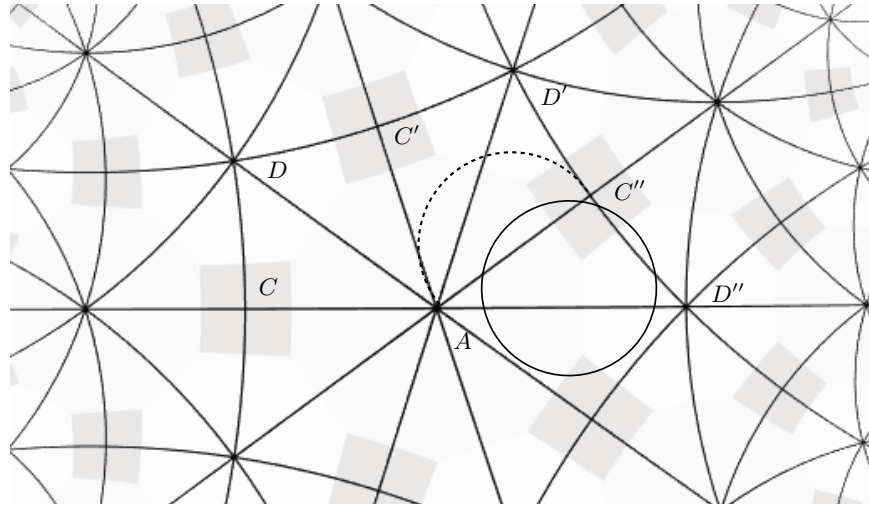


FIGURE 14. The view from the truncated vertex of type $(2, 4, 5)$.

D'' in its interior. But such a circle can have no points in the hyperbolic polygon $CAD''C''D'C'D$ that lie outside of the union of triangle $AC''D''$ and the circle with the segment AC'' as its diameter (pictured with a dashed arc in the figure). Consequently, this circle cannot meet any of the sides of this hyperbolic polygon other than AD'' and $D''C''$, and, in particular, we have $\Pi_1 \cap \Pi_2 = \emptyset$. An analogous argument works whenever B has hyperbolic type with one incident order 2 edge and $l \geq 4$.

The case when $l \geq 4$ and B has hyperbolic type with no incident order 2 edge is similar. See Figure 15, in which Π_2 is represented by the semicircular arc CD and Π_1 is represented as the circle pictured. When $l \geq 4$, we observe that, in any similar picture (for example, Figure 16), the angles α and β will always be at least $\pi/2$. Consequently, because the center of the circle representing Π_1 is contained in the hyperbolic triangle AEF , this circle will be disjoint from the segment AD . Also,

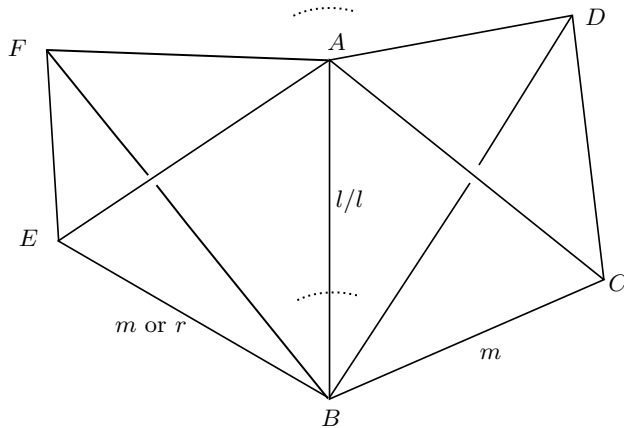
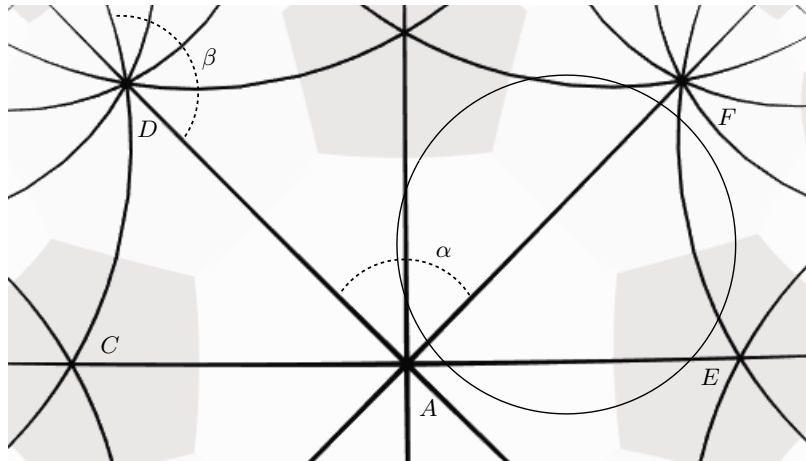


FIGURE 15. The view from the truncated vertex of generic hyperbolic type when none of l , m and r is 2.

noting that AD will always have Euclidean length equal to one of the lengths $|AF|$ or $|AE|$, it is easily seen that no point of the circle CD that lies above the line AD can be closer to the center of the circle representing Π_1 than any of the points A , E or F . We conclude that $\Pi_1 \cap \Pi_2 = \emptyset$ in this case.

4.2. The case when multiple edges separates e_1 from e_2 : Recall that $\Pi_{\mathcal{T}}$ denotes the plane stabilized by a copy of a triangle subgroup in the fundamental group of \mathcal{O}_T , and that e_1 and e_2 denote the translates of two edges of T that lie in the plane Π_F corresponding to the development in \mathbb{H}^3 of one face F of T and whose intersections with $\Pi_{\mathcal{T}}$ correspond to two of the cone points of the immersed turnover whose fundamental group stabilizes $\Pi_{\mathcal{T}}$. Now that we have determined the conditions on T which give rise to a turnover in \mathcal{O}_T when $\Pi_{\mathcal{T}}$ intersects a single edge in the development of F between e_1 and e_2 , we will show that it is impossible for there to be more

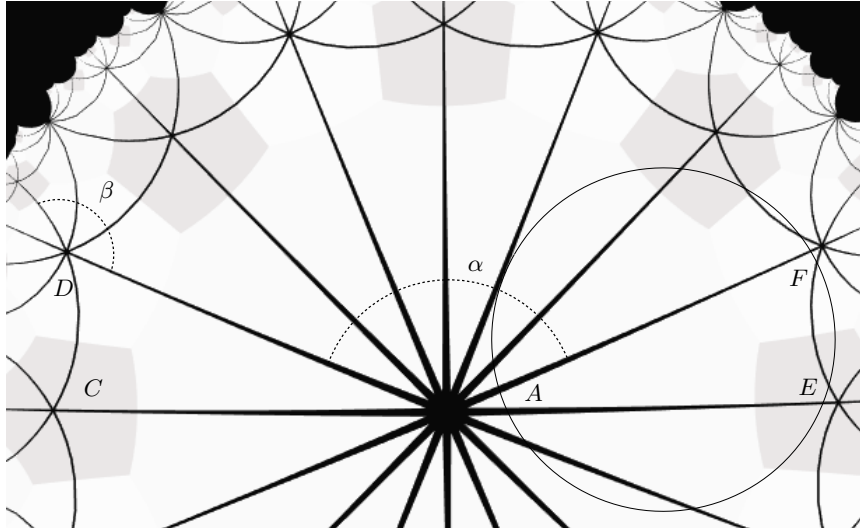


FIGURE 16. Another view from the truncated vertex of generic hyperbolic type when none of l , m and r is 2.

than one such edge in the development of F between e_1 and e_2 . This will complete the classification of immersed turnovers in tetrahedral orbifolds all of whose vertices are generalized.

Figure 17 shows two possible schematic diagrams for this discussion. In each of the subfigures, the edges e_1 and e_2 are indicated, and the dashed line represents the intersection of $\Pi_{\mathcal{T}}$ with Π_F . Notice that, in each triangle of the planar development of F , there is always a unique translate of a vertex of T that is separated from the other two by $\Pi_{\mathcal{T}}$. The edge translates of T labeled by “ s ” represent points at which this vertex switches. We consider the following procedure for dividing any diagram of the type from Figure 17 into subdiagrams of the type (up to possible reflection or order two rotation) given in Figures 18 and 19:

- (1) Starting at the first edge of the diagram, we follow the ray corresponding to the intersection of $\Pi_{\mathcal{T}}$ with this plane until we arrive at the first switch. There must always be such a switch, for otherwise the supposed turnover would be parallel to a generalized vertex of T .
- (2) If the switch is the only switch in the diagram, then our diagram looks like, up to reflection or rotation, one of the diagrams from Figure 18. In this case, we stop.
- (3) If there is more than one switch and the diagram looks like, up to reflection or rotation, one of the diagrams from Figure 19, then we stop.
- (4) If we have not halted in the previous two steps, then the diagram up to and including the first edge after the switch looks like the diagram in either Figure 18(a) or 18(b). Call this portion a *subdiagram*.

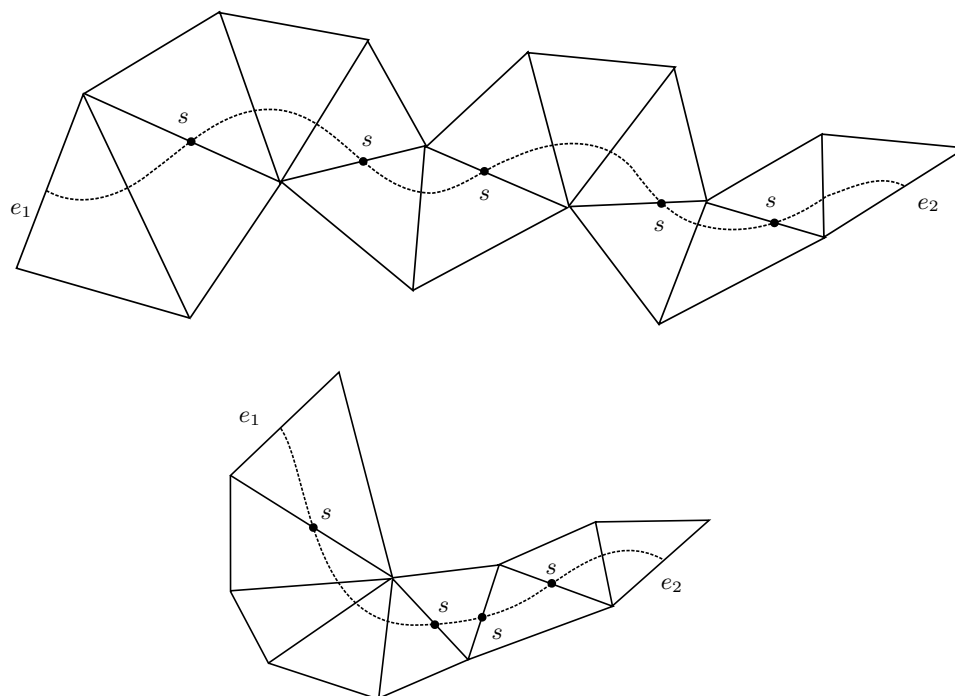


FIGURE 17. Schematic of some possible developments of a face of T , together with switches and the possible intersection of the plane $\Pi_{\mathcal{T}}$.

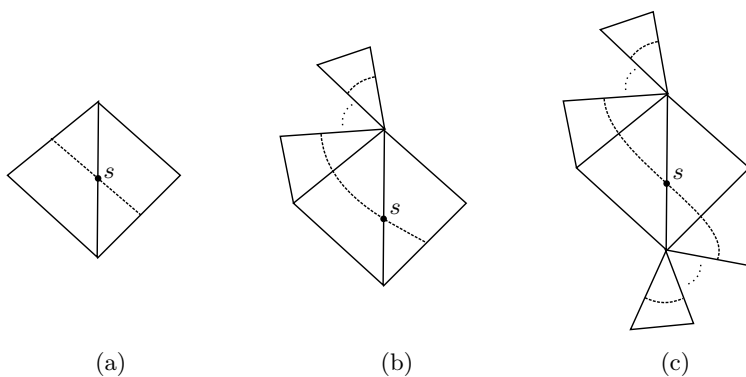


FIGURE 18. One type of possibility for the subdiagram components for a diagram of the type given in Figure 17.

- (5) Starting at the last edge of the subdiagram from the previous step, we repeat this process with the remaining portion of the original diagram, starting from the first step, until we reach edge e_2 .

This procedure divides our diagram into subdiagrams of the type illustrated in Figure 18(a) and 18(b), with the possible exception that the final subdiagram may be of the type in Figure 18(c) or one of the two types in Figure 19. Again, we denote by Π_1 and Π_2 the planes at e_1 and e_2 , respectively, whose intersections with $\Pi_{\mathcal{T}}$ are supposed

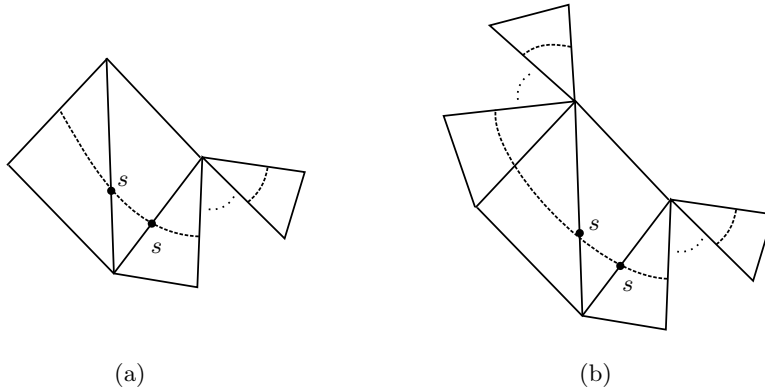


FIGURE 19. Another type of possibility for the subdiagram components for a diagram of the type given in Figure 17.

to form two of the sides of a triangle in the tiling of $\Pi_{\mathcal{T}}$. Our strategy is to use the subdiagrams of Figures 18 and 19 to find a sequence of planes in \mathbb{H}^3 —one or more planes at each of the two outer-most edges of each subdiagram—that are pairwise disjoint on either side of Π_F and that therefore separate Π_1 from Π_2 .

Notation. We make the following language and notational conventions: For the remainder of the paper, Π_F refers to the plane in which all of the diagrams from Figures 17, 18 and 19 reside. We also use L_F to denote the line segment in these diagrams that represents the intersection of $\Pi_{\mathcal{T}}$ with Π_F . Additionally, the phrase “the other side of Π_F ” refers to side of Π_F that is behind the page (relative to the reader), and the use of the word “plane” at any edge in a diagram always refers to one of the planes in the tiling of \mathbb{H}^3 that passes through that edge (i.e., a translate by an element of the orbifold fundamental group of \mathcal{O}_T of one of the planes corresponding to a face of T).

We first make two observations about the subdiagram from Figure 18(a). First, if either of the orders of the two edges separated by the switch is 2, then no plane at either edge can meet any of the planes at the other edge (excepting the plane Π_F). This fact follows from the extensive analysis done in Subsection 4.1. Second, if the two planes at the outer edges that are inclined closest toward the switch do meet (thus generating an immersed turnover in \mathcal{O}_T with two singular points of order at least 6 and one singular point of order at least 3), then the next two planes (one at either outer edge) inclined away from the switch do not meet. This fact follows from an easy analysis of the patterns of line intersections in hyperbolic triangular tilings. See Figure 20 for the conditions on the vertex orders of an (a, b, c) hyperbolic triangular tiling under which such intersections can occur (in particular, one of the vertices must have order 2, which does not happen in our situation).

Therefore, it is left to show that, for each of the remaining types of subdiagram, the two planes at the outer-most edges that are inclined closest to the single or double switch in the subdiagram (where by “inclined closest” we mean closest on the other side of Π_F to the planes passing through the switch edge(s)) do not intersect. This

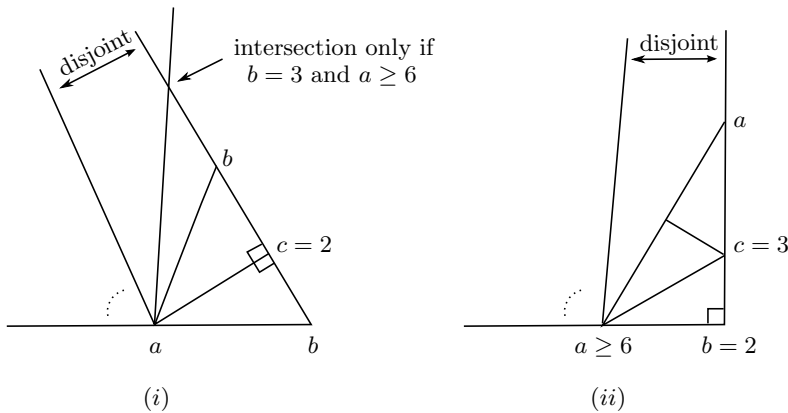


FIGURE 20. The possibilities for the intersection of lines in a triangular tiling of \mathbb{E}^2 or \mathbb{H}^2 .

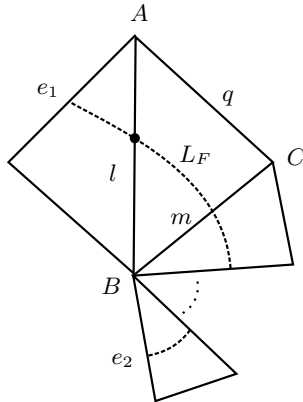


FIGURE 21. The case of Figure 18(b).

will produce the sequence of planes that separates Π_1 and Π_2 , and therefore complete the proof. We will show this by cases, which are indicated by their labels in the figures.

4.2.1. *18(b)*: See Figure 21, in which we have supposed without loss of generality that F is the face ABC of the tetrahedron T , as in Figure 9. This picture is symmetric with Figure 18(b) by a 180° rotation. Observe that the edges incident at the vertices A and B have orders l, q, p and l, m, r (respectively).

We observe that the vertex B must have at least one order 2 edge incident to it. Otherwise, if B were of the type (x, y, z) with all orders at least 3, then it is easily shown, using the information from Figure 20, that Π_2 (the plane inclined closest to the switch at edge e_2) cannot meet the plane at edge BC that is inclined closest to the switch. Furthermore, by our analysis in the cases of Subsection 4.1, the only way that Π_1 can meet the plane through edge BC that is inclined closest to the switch is

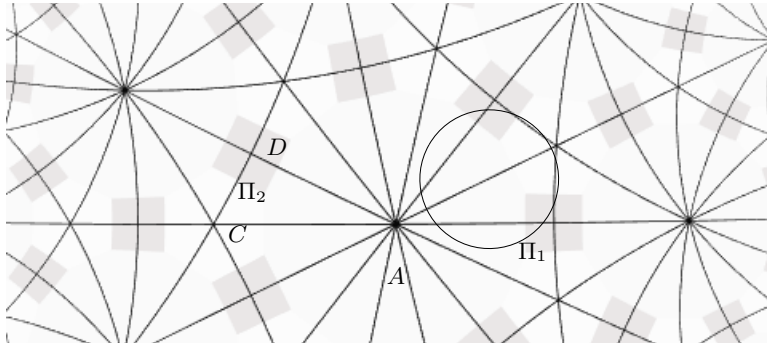


FIGURE 22. A view from the truncated vertex of hyperbolic type $(2, 3, 7)$.

if B has an incident order 2 edge. Consequently, if there is no such order 2 edge at B , then we have $\Pi_1 \cap \Pi_2 = \emptyset$.

So B either has the type $(2, 3, x \geq 6)$ or $(2, y \geq 4, z \geq 4)$. In the latter case, if $l = y$ or $l = z$, then we have shown in Subsection 4.1.3 that Π_1 is disjoint from every plane through edge BC . It is then a simple exercise, using Figure 20, to show that there is no plane through any of the subsequent edges toward e_2 which L_F crosses that meets the plane through edge BC that is inclined closest to the switch. So $\Pi_1 \cap \Pi_2 = \emptyset$ in this case. In the latter case and when $l = 2$ and $y = 4 = z$, we may show that $\Pi_1 \cap \Pi_2 = \emptyset$ by using the Euclidean vertex argument as in Figure 13. In the latter case and when $l = 2$ and one of y or z is greater than 4, it is again easily shown that the second closest plane to the switch through edge BC (recall that Π_1 must be disjoint from this plane) misses the plane inclined closest to the switch at every subsequent edge that L_F crosses toward e_2 .

This leaves us with the possibility that B has type $(2, 3, x \geq 6)$. When $l = x$, then we are in a case that is similar to the first case in Section 4.1.3, i.e., we have to consider a regular l -gon in either the Euclidean or hyperbolic plane and a circle centered inside the polygon that does not contain in its interior the center of the polygon, any vertex of the polygon or any midpoint of a side. In this case, however, we observed that such a circle (representing Π_1) must be disjoint from all but two sides of the polygon. But the plane Π_2 will correspond in such a picture to a line or circular arc in the picture that does not meet the interior of this polygon, and so $\Pi_1 \cap \Pi_2 = \emptyset$ when $l = x$. See Figure 22 for an example illustration of this argument, in the case when $x = 7$.

The cases when $l = 2$ or $l = 3$ remain. In the case when $l = 3$, we refer to Figure 23. In this picture, Π_1 is represented by a circle centered inside the triangle $AC'D'$ that cannot meet any vertex of the triangulation and that can only meet the sides AD and AD' of the x -gon centered at C' . Since Π_2 would have to be represented by a line emanating from a vertex on the line CAD which is further to the left than C , and no such lines will enter the x -gon centered at C' , we conclude that $\Pi_1 \cap \Pi_2 = \emptyset$ in this case.

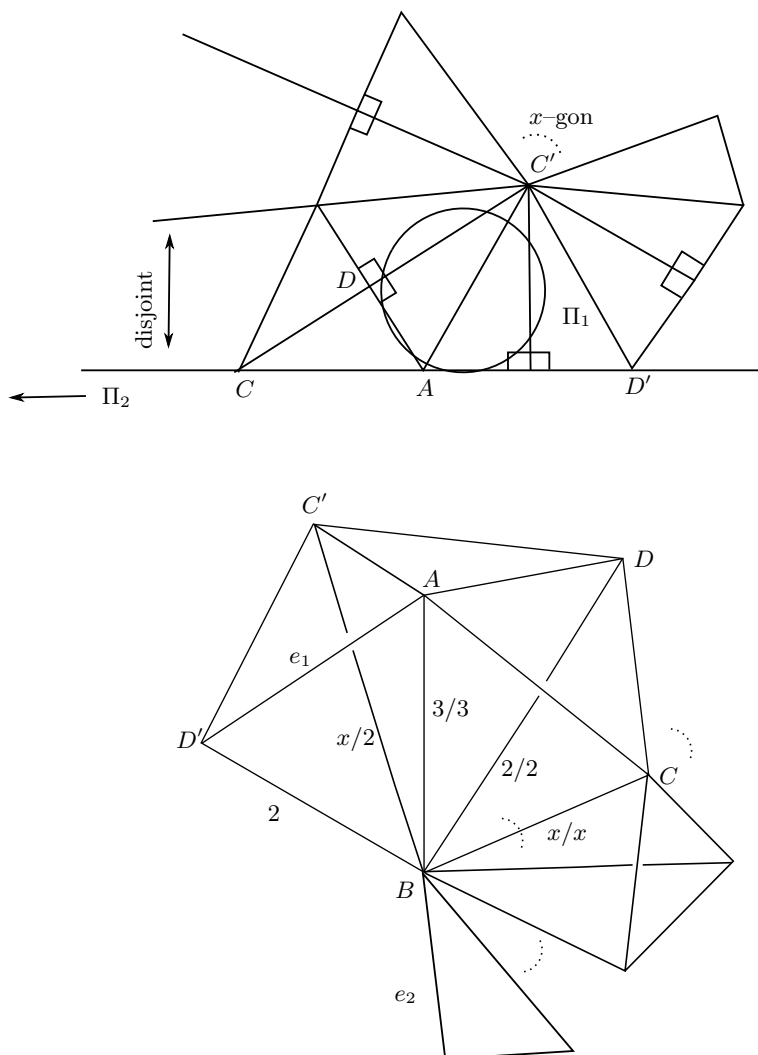


FIGURE 23. A view from the truncated vertex of type $(2, 3, x \geq 6)$.

When $l = 2$, then the only way for which we are unable to apply the preceding argument is when $m = 3$. See Figure 24. The reason is that it may be that the angle $\angle A'DC'$ is less than $\pi/2$, and so it is, in principle, possible that the circle representing Π_1 may intersect the line represented Π_2 if the latter is the line $A'D'$ (we have drawn the circle as an ellipse in order to indicate this possible intersection). However, using the accompanying tetrahedral illustration and the techniques of Subsection 4.1 (applied to vertex D), it is easily shown that p must equal 2 in order for Π_1 and Π_2 to intersect. This cannot occur, as $l = 2$ and we are assuming that T has no finite vertices. (The resulting (q, x, x) hyperbolic turnover that results in this finite vertex case is accounted for in the conjectural classification at the conclusion of the paper.)

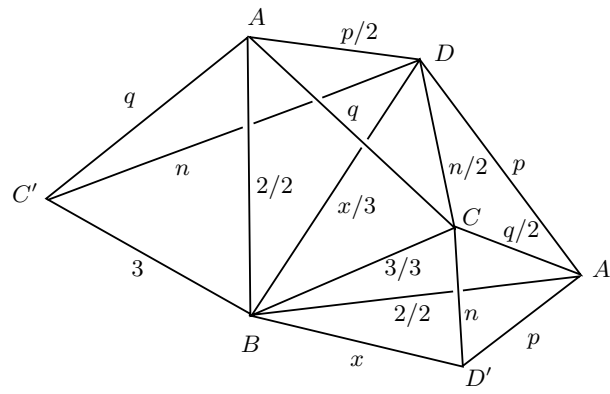
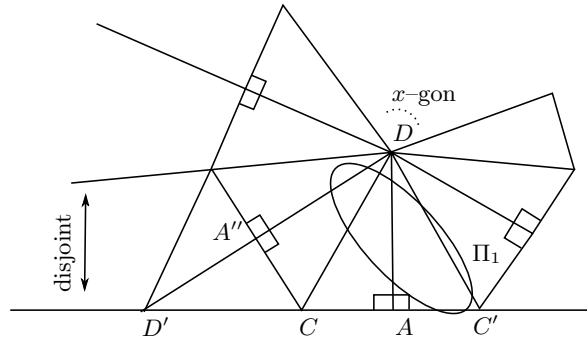


FIGURE 24. A view from the truncated vertex of type $(2, 3, x \geq 6)$.

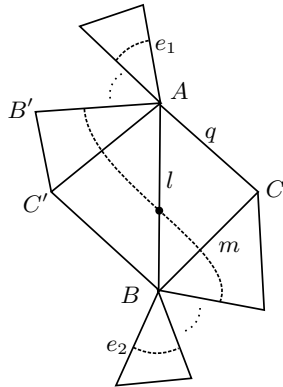


FIGURE 25. The case of Figure 18(c).

4.2.2. *18(c)*: See Figure 25, in which again we have supposed without loss of generality that F is the face ABC of the tetrahedron T , with the edges incident at the vertices A and B having orders l, q, p and l, m, r (respectively). We again denote by the Π_1 and Π_2 the planes at the edges e_1 and e_2 , respectively, that are inclined closest to the switch edge. By the previous case, we know that Π_1 meets none of

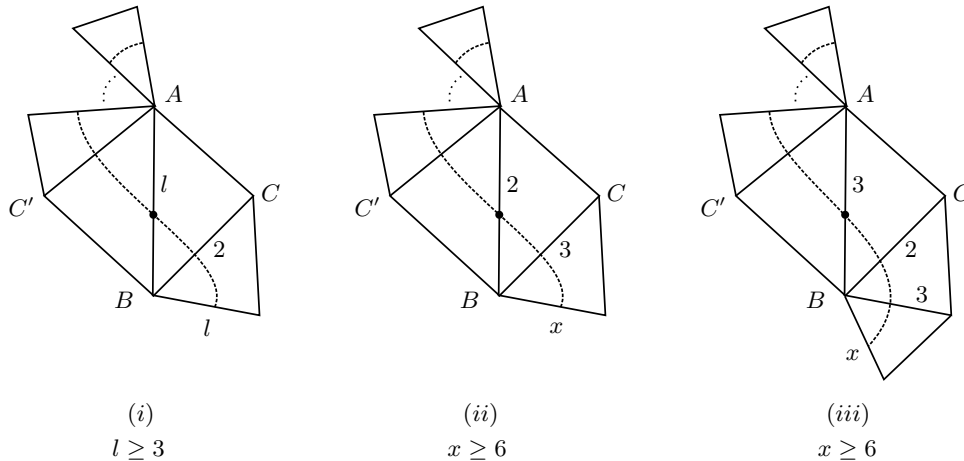


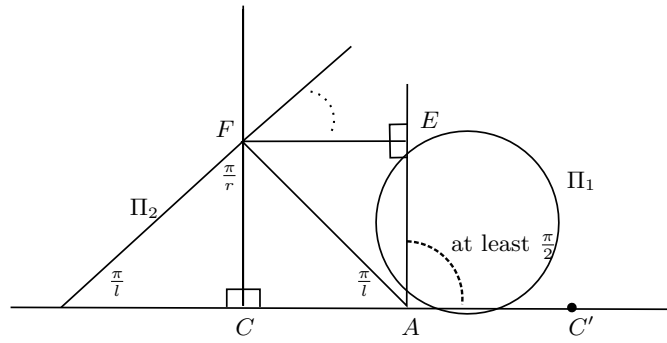
FIGURE 26. After analysis, the remaining cases of Figure 18(c).

the planes through edge BC . It is therefore necessary, if Π_1 and Π_2 are to intersect, that Π_2 cross every plane through edge BC . As in the previous case, then, we can conclude that one of the edges incident at B must have order 2. Using Figure 20, we can reduce the cases that must be ruled out to those listed in Figure 26. If we can show that no intersections occur in each of these cases, then it is not difficult to see that no further intersections can occur if, for instance, Π_2 emanates from an edge that is further along from the switch than the furthest edge in each of these diagrams.

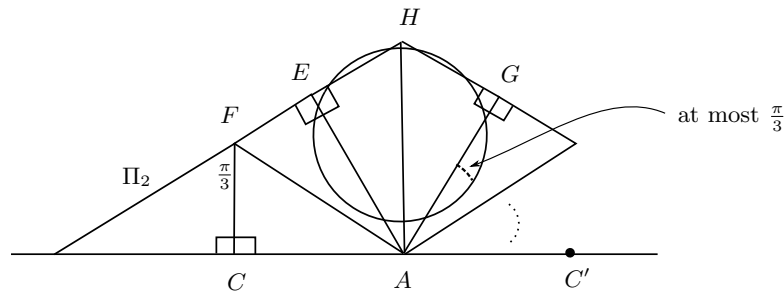
We begin with case (i). If $l \geq 4$, then it is not possible for Π_1 to meet the plane through the switch that is inclined closest to the edge BC . But Π_1 must meet some of the planes through the switch and it must meet the plane Π_F . So the picture must be as in Figure 27(a). The indicated circle represents Π_1 in the figure, and we are assuming for time being that $r \geq 4$. Because the angle $\angle C'AE$ is at least $\pi/2$, it is not possible for the circle to intersect the segment EF . Consequently, because $r > 3$, we have that the circle cannot meet the line segment that represents Π_2 . If $r = 3$, then $l \geq 6$ and we refer to Figure 27(b). In order for the circle representing Π_1 to meet the line representing Π_2 , it is necessary for the circle to be centered in the quadrilateral $AHFG$. In particular, it must make an angle of no more than $\pi/3$ with the line segment AG . But angle $\angle C'AG$ is at least $\pi/3$, and so it is not possible for the circle to intersect both the line segments EH and AC' .

The case (i) and when $l = 3$, as well as cases (ii) and (iii), follow by straightforward applications of the techniques we have previously employed in this subsection.

4.2.3. *19(a)*: See Figure 28. We must first address the case when $e_2 = A'C$. There are two possibilities that we must consider in determining whether or not Π_1 and Π_2 can intersect: either (1) Π_1 meets the plane through BC that is closest in inclination to the switch edge AB (it cannot meet more planes through BC , by our previous observations) and Π_2 meets at least the second closest plane through BC to the



(a)



(b)

FIGURE 27. One case of Figure 18(c).

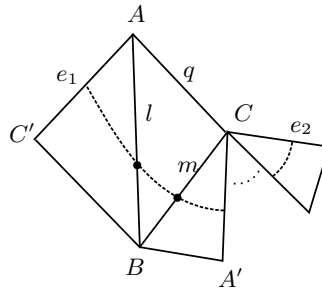


FIGURE 28. One case of Figure 19(a).

switch edge AB , or (2) Π_1 meets no planes passing through BC and Π_2 meets all of the planes passing through BC . We handle these two cases below:

- (1) In order for Π_1 to meet a plane passing through BC , our tetrahedron must take one of the forms of items (1)–(3) at the conclusion of the paper. We consider the case when $l = 3$, corresponding to item (3) in the summary (the other cases are similar, or else use circle arrangements in the Poincaré disk as in the previous subsections). If $l = 3$, then $q = 2$, $m \geq 6$ and n (the order of the third edge associated to vertex C) is at least 3. It is then an easy analysis,

using Figure 20, to see that there is no choice of n and m for which Π_2 can intersect the plane either of the two closest planes through BC toward the edge AB . This rules out any possible intersection of Π_1 with Π_2 for case (1).

- (2) If the order of edge BC is greater than 4, then it is not possible to choose integers for the type of vertex C so that Π_2 crosses all the planes through BC . The same statement is true if the order of BC is 3 and the vertex C has no incident order 2 edge. So the order of edge BC is either 3 and C has the type $(2, 3, x \geq 6)$ or the order of edge BC is 2. In the former case, it can be shown using our previous circle arrangement arguments that $\Pi_1 \cap \Pi_2 = \emptyset$. In the latter case, we may use exactly the same argument given for case (i) of Figure 26 given in section 4.2.2.

So we can now assume $e_2 \neq A'C$. We observe that removing the sides AC' and BC' from the diagram leaves a picture that is equivalent to the previous case of Subsection 4.2.1. In this case, we therefore know that Π_2 misses every plane through the switch edge AB . This forces l to be either 2 or 3, in order for Π_1 to cross every plane through this switch edge. Moreover, we must have, as in previous cases, that the type of vertices A and C must include an order 2 point. Suppose $l = 2$. This implies that neither m nor q is 2. If, in addition, neither m nor q is 3, then it is straightforward using the information in Figure 20 to show that Π_2 cannot meet the plane through $A'C$ inclined closest to Π_1 , and so prove that $\Pi_1 \cap \Pi_2 = \emptyset$ in this case. So either $m = 3$ and $q \geq 6$ or $q = 3$ and $m \geq 6$. In the either case, it is a straightforward application of the techniques already employed to show that Π_1 and Π_2 do not intersect.

Now suppose $l = 3$. Because Π_1 must cross every plane through the switch edge AB , this forces the order of edge e_1 to be at least 6 and $q = 2$. This implies that, if $m = 3$, then the order of the edge $A'C$ is also at least 6, in which case it is not possible for either Π_1 or Π_2 to meet the plane through $A'C$ that is inclined closest to the switch edge AB . So we must have $m \geq 6$. But now Π_1 will not meet the plane through BC that is second-closest inclined toward edge AB , and if $m \geq 7$, then it is readily seen (using the information in Figure 20) that Π_2 cannot intersect this second closest inclined plane, either. So we are left with $m = 6$. However, this case is easily handled using the techniques of the previous subsections.

4.2.4. *19(b)*: See Figure 29. Using our previous results, we conclude that it is not possible for Π_2 to meet any of the planes through the edge AC' . Consequently, the intersection of Π_1 and Π_2 can only occur if Π_1 crosses every plane through this edge. The subsequent possibilities and arguments to rule them out are all straightforward to carry out, using the techniques we have employed to this point. This completes the proof. 1.2

Summary. We provide a summary of the classification of immersed turnovers in the orbifold \mathcal{O}_T associated to the generalized tetrahedron $T[l, m, q; n, p, r]$. These are listed in coordination of the flow of the proof, but symmetric cases are indicated

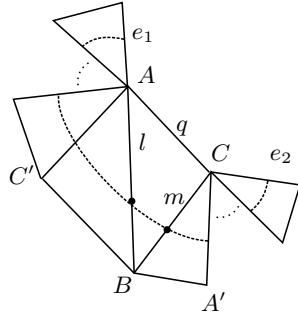


FIGURE 29. One case of Figure 19(b).

(the 24 symmetric cases are determined by applying an element of the symmetric group S_4 : any element of the symmetric group S_3 may be applied to both the first and second triples of $T[l, m, q; n, p, r]$, and any pair from one triple may be swapped with the corresponding pair of the other triple). We also include a conjectural list of all the immersed turnovers in hyperbolic tetrahedral orbifolds. All of these can be confirmed using the techniques of this paper, and while the author believes this list to be exhaustive, the necessary computations to determine the complete classification are somewhat extensive.

- (1) $T[2, m, q; 2, p, 3]$. \mathcal{O}_T contains an immersed (q, m, p) turnover, where $q \geq 3, m \geq 6$ and $p \geq 6$.
- (2) $T[2, m, q; 2, 3, r]$ (symmetric to item (1)). \mathcal{O}_T contains an immersed (q, m, r) turnover, where $q \geq 6, m \geq 3$ and $r \geq 6$.
- (3) $T[3, m, 2; n, p, 2]$ (symmetric to item (1)). \mathcal{O}_T contains an immersed (m, n, p) turnover, where $m \geq 6, n \geq 3$ and $p \geq 6$.

Conjectural list of all immersed turnovers in hyperbolic tetrahedral orbifolds:

- (4) $T[2, m, q; 2, p, 3]$. \mathcal{O}_T contains an immersed (q, m, p) turnover for any of the following values:
 - (a) $q = 2, m = 4$ and $p \geq 5$. In this case, \mathcal{O}_T also contains
 - (i) a $(2, p, p)$ turnover,
 - (ii) a $(4, 4, 5)$ turnover if $p = 5$, and
 - (iii) a $(p/2, p, p)$ turnover if p is even.
 - (b) $q = 2, p = 4$ and $m \geq 5$ (symmetric to item (4), with the same set of additional non-maximal turnovers).
 - (c) $q = 2, m \geq 5$ and $p \geq 5$. In this case, \mathcal{O}_T also contains
 - (i) a $(m, m, p/2)$ turnover if p is even, or
 - (ii) a $(m/2, p, p)$ turnover if m is even.
 - (d) q, m and p are all greater than 2, and at least one is greater than 3. In this case, if two of the values are 3, then \mathcal{O}_T also contains a (x, x, x) turnover, where x is the integer that is greater than 3.
- (5) $T[3, 2, 2; 2, p, 3]$. \mathcal{O}_T contains an immersed $(2, p, p)$ turnover, where $p \geq 5$.

- (6) $T[3, m, 2; 2, p, 3]$. \mathcal{O}_T contains an immersed (m, p, p) turnover, where $m \geq 3$ and $p \geq 4$.
- (7) $T[3, m, 3; 2, 3, 2]$. \mathcal{O}_T contains an immersed $(3, m, m)$ turnover, where $m \geq 4$.
- (8) $T[4, 3, q; 2, 2, 2]$. \mathcal{O}_T contains an immersed $(q, q, 3)$ turnover, where $q \geq 4$.
- (9) $T[2, 2, 4; n, 3, r]$. \mathcal{O}_T contains an immersed turnover of type $(2, 4, r \geq 5)$ (as well as the additional non-maximal turnovers listed in item (4)) if $n = 2$, an immersed turnover of type $(4, 4, r \geq 3)$ if $n = 3$, and immersed turnovers of types $(3, 3, 5)$, $(3, 5, 5)$ and $(5, 5, 5)$ if $n = 2$ and $r = 5$.
- (10) $T[2, 3, q; 2, 3, r]$. \mathcal{O}_T contains an immersed (q, r, r) turnover, where $q \geq 3$ and $r = 4$ or $r = 5$.
- (11) $T[2, 2, q; 3, 5, 2]$. \mathcal{O}_T contains an immersed $(q, q, 5)$ turnover, where $q \geq 3$.
- (12) $T[2, 2, 5; 2, 3, 5]$. \mathcal{O}_T contains an immersed $(3, 5, 5)$ turnover.
- (13) $T[2, 2, 3; 3, p, 2]$. \mathcal{O}_T contains immersed turnovers of type $(3, p, p)$ and (p, p, p) , where $p = 5$ or $p = 6$ (also, $(2, p, p)$ by item (5) and $(3, 3, 5)$, when $p = 5$, by item (11)).
- (14) $T[2, 2, 3; 2, p, 3]$. \mathcal{O}_T contains immersed turnovers of type $(2, p, p)$, $(3, 3, p)$ and (p, p, p) if $p = 5$, and an immersed turnover of type $(3, p, p)$ if $p = 6$.

REFERENCES

- [1] Colin Adams and Eric Schoenfeld, *Totally geodesic Seifert surfaces in hyperbolic knot and link complements. I*, Geom. Dedicata **116** (2005), 237–247. MR 2195448
- [2] E. M. Andreev, *Convex polyhedra in Lobachevskii spaces*, Mat. Sb. (N.S.) **81** (**123**) (1970), 445–478. MR 0259734
- [3] ———, *Convex polyhedra of finite volume in Lobachevskii space*, Mat. Sb. (N.S.) **83** (**125**) (1970), 256–260. MR 0273510
- [4] Michel Boileau, Sylvain Maillot, and Joan Porti, *Three-dimensional orbifolds and their geometric structures*, Panoramas et Synthèses [Panoramas and Syntheses], vol. 15, Société Mathématique de France, Paris, 2003. MR 2060653
- [5] Daryl Cooper, Craig D. Hodgson, and Steven P. Kerckhoff, *Three-dimensional orbifolds and cone-manifolds*, MSJ Memoirs, vol. 5, Mathematical Society of Japan, Tokyo, 2000, With a postface by Sadayoshi Kojima. MR 1778789
- [6] William D. Dunbar, *Hierarchies for 3-orbifolds*, Topology Appl. **29** (1988), no. 3, 267–283. MR 953958
- [7] Craig D. Hodgson, *Deduction of Andreev’s theorem from Rivin’s characterization of convex hyperbolic polyhedra*, Topology ’90 (Columbus, OH, 1990), Ohio State Univ. Math. Res. Inst. Publ., vol. 1, de Gruyter, Berlin, 1992, pp. 185–193. MR 1184410
- [8] C. Maclachlan, *Triangle subgroups of hyperbolic tetrahedral groups*, Pacific J. Math. **176** (1996), no. 1, 195–203. MR MR1433988 (98d:20056)
- [9] Bernard Maskit, *Kleinian groups*, Grundlehren der Mathematischen Wissenschaften [Fundamental Principles of Mathematical Sciences], vol. 287, Springer-Verlag, Berlin, 1988. MR 959135
- [10] John W. Morgan, *On Thurston’s uniformization theorem for three-dimensional manifolds*, The Smith conjecture (New York, 1979), Pure Appl. Math., vol. 112, Academic Press, Orlando, FL, 1984, pp. 37–125. MR 758464
- [11] Shawn Rafalski, *Immersed turnovers in hyperbolic 3-orbifolds*, Groups Geom. Dyn. **4** (2010), no. 2, 333–376. MR 2595095
- [12] John G. Ratcliffe, *Foundations of hyperbolic manifolds*, Graduate Texts in Mathematics, vol. 149, Springer-Verlag, New York, 1994. MR 1299730
- [13] Roland K. W. Roeder, John H. Hubbard, and William D. Dunbar, *Andreev’s theorem on hyperbolic polyhedra*, Ann. Inst. Fourier (Grenoble) **57** (2007), no. 3, 825–882. MR 2336832
- [14] David Singerman, *Finitely maximal Fuchsian groups*, J. London Math. Soc. (2) **6** (1972), 29–38. MR MR0322165 (48 #529)
- [15] W. P. Thurston, *The geometry and topology of 3-manifolds*, Lecture notes from Princeton University, 1978–80.
- [16] William P. Thurston, *Three-dimensional manifolds, Kleinian groups and hyperbolic geometry*, Bull. Amer. Math. Soc. (N.S.) **6** (1982), no. 3, 357–381. MR 648524

- [17] Akira Ushijima, *A volume formula for generalised hyperbolic tetrahedra*, Non-Euclidean geometries, Math. Appl. (N. Y.), vol. 581, Springer, New York, 2006, pp. 249–265. MR 2191251
- [18] J. Weeks, *Kaleidotile*, <http://www.geometrygames.org/KaleidoTile/>.

DEPARTMENT OF MATHEMATICS AND COMPUTER SCIENCE, FAIRFIELD UNIVERSITY, FAIRFIELD, CT 06824, USA
E-mail address: `srafalski@fairfield.edu`